Journal of Solid State Chemistry 292 (2020) 121703

Contents lists available at ScienceDirect

Journal of Solid State Chemistry

journal homepage: www.elsevier.com/locate/jssc

Coloured intermetallic compounds $LiCu_2Al$ and $LiCu_2Ga$

Vidyanshu Mishra [a], Abishek K. Iyer [a], Dundappa Mumbaraddi [a], Anton O. Oliynyk [a,b], Guillaume Zuber [a], Aurélien Boucheron [a], Grygoriy Dmytriv [c], Guy M. Bernard [a], Vladimir K. Michaelis [a], Arthur Mar [a,*]

[a] Department of Chemistry, University of Alberta, Edmonton, Alberta, T6G 2G2, Canada
[b] Department of Chemistry and Biochemistry, Manhattan College, Riverdale, NY, 10741, United States
[c] Department of Inorganic Chemistry, Ivan Franko National University of Lviv, 79005, Lviv, Ukraine

ARTICLE INFO

Keywords:
Intermetallic compounds
Optical properties
Electronic structure
NMR spectroscopy

ABSTRACT

The Li-containing intermetallic compounds $LiCu_2Al$ and $LiCu_2Ga$ were prepared by induction heating. Powder X-ray diffraction revealed cubic structures for these compounds: $Li_{0.5}CuAl_{0.5}$, CsCl-type ($Pm\bar{3}m$, $Z = 1$, $a = 2.9283$ (2) Å); $LiCu_2Ga$, Heusler or Cu_2MnAl-type ($Fm\bar{3}m$, $Z = 4$, $a = 5.8617$ (4) Å). Solid-state ^7Li NMR spectra confirmed that the Li atoms are situated on a single site rather than being disordered over multiple sites. Optical reflectance spectra show absorption edges in the visible region consistent with the appearance of colour in these compounds: red for $LiCu_2Al$, yellow for $LiCu_2Ga$. Band structure calculations revealed the presence of completely filled Cu 3d states, and suggest that interband transitions from the top of this narrow band (located around 2.5 eV below the Fermi level) to empty bands are responsible for the colour.

1. Introduction

Metallic substances, which encompass many elements, alloys, and intermetallic compounds, possess varied physical and chemical properties which make them useful in many applications such as structural, magnetic, superconducting, and catalytic materials. Among these properties, however, colour is unusual and highly prized, as exemplified by the widespread use of gold (as well as various alloys with copper, silver, and other metals) in jewellery and decorative coatings, a multibillion dollar global industry [1–6]. Apart from gold and its alloys, intermetallic compounds can also exhibit colour, but exceedingly rarely: out of 10^5–10^6 known intermetallic compounds, only ~10^2 have been reported to be coloured [7,8]. They include binary (e.g., dark blue $CoSi_2$ [9], purple $AuAl_2$ ("purple plague") [10–12], yellow $PtAl_2$ [13], red PdIn [14], light yellow $MgCu_2$ [15]), ternary (various Li- or Mg-containing intermetallics) [16–19], and quaternary phases (e.g., LiMgPdSn) [16].

Given the presence of highly delocalized electrons, typical metallic substances have uniformly high optical reflectivity in the visible region of the electromagnetic spectrum, resulting in their characteristic lustrous appearance. In contrast, the few exceptions that exhibit colour do so because they have absorption edges that fall within the visible region, corresponding to electronic transitions in the range of 1.5–3.0 eV. The electronic conditions for the appearance of colour can be related to chemical and structural features: (i) the presence of sharp peaks in the density of states (DOS), which lead to distinct absorption edges, requires high space group symmetry; (ii) the placement of the Fermi level such that these states with high DOS are completely filled, generally requires late transition metals; and (iii) the fulfilment of the dipole selection rule ($\Delta l = \pm 1$) requires strong mixing of metal d and metalloid s/p states [7,8]. It is not a coincidence that many previously known coloured intermetallics are Zintl phases with cubic structures, because they are a special class of intermetallic compounds that satisfy normal valence rules, resulting in the presence of a pseudogap in the DOS that separate filled bonding from empty antibonding levels [16–19]. This situation can be contrasted with semiconductors, which exhibit colour because there is a finite energy gap, not a pseudogap, in the DOS.

The majority of known coloured intermetallics contain precious metals (e.g., Pd, Pt, Ag, Au), usually in combination with Li or Mg. The appearance of colour in such compounds was typically noted as a side observation and not a targeted property. It would be desirable to discover new coloured intermetallics prepared with less expensive components, through a more directed approach with an aim to understand how the colour arises from structural and electronic features. We hypothesize that the ternary systems Li–Cu–X (X = group 13–15 metals or metalloids)

* Corresponding author.
E-mail address: arthur.mar@ualberta.ca (A. Mar).

https://doi.org/10.1016/j.jssc.2020.121703
Received 11 July 2020; Received in revised form 25 August 2020; Accepted 30 August 2020
Available online 2 September 2020

may be fruitful to find such compounds, given the requirements described above. Inspection of these systems reveals several existing coloured intermetallics (Table S1 in Supplementary Data), such as $LiCu_2Si$, $LiCu_2Ge$, Li_2CuGe, and Li_2CuSn [20], suggesting that more can be expected.

Here we report the preparation of $LiCu_2Al$ and $LiCu_2Ga$, their structural characterization by powder X-ray diffraction, and their optical reflectance spectra. ^{7}Li nuclear magnetic resonance spectroscopy was performed to resolve ambiguities in locating the Li atoms, which scatter X-rays weakly, by diffraction methods alone. Electronic structure calculations were also carried out to gain insight on the origin of colour in these compounds.

2. Experimental

2.1. Synthesis

Starting materials were Li rod (99.5%, Cerac), Cu shot (99.5%, Alfa Aesar), Al powder (99.97%, Cerac), and Ga ingot (99.99% Alfa Aesar). All manipulations were performed in an argon-filled glove box. The Li rod was scraped to remove surface oxides prior to use and cut into pieces of the desired mass. Mixtures of Li, Cu, and Al or Ga were combined in a molar ratio of 1:2:1 in a total mass of 0.200 g and placed within tantalum tubes, which were welded shut in a Centorr 5 TA tri-arc furnace on a water-cooled copper hearth under an argon atmosphere. The samples were placed in a water-cooled Ambrell EASYHEAT 5060LI 6.0 kW induction heater where they were subjected to a frequency of 157 kHz and a current of 138 A for 18 min under argon atmosphere within a copper coil of 5-cm diameter. Based on optical pyrometer measurements, the temperature attained was estimated to be between 800 and 900 °C. These are the optimum conditions that yield the most consistent results in terms of phase purity and uniform colour.

2.2. Characterization

Energy-dispersive X-ray (EDX) analysis on the products, which were examined on a JEOL JSM-6010LA scanning electron microscope, confirmed the 2:1 ratio of Cu to Al or Ga, but Li is undetectable by this technique. Powder X-ray diffraction (XRD) patterns were collected on an Inel diffractometer equipped with a curved position-sensitive detector (CPS 120) and a Cu $K\alpha_1$ radiation source operated at 40 kV and 20 mA. The patterns were analyzed using the program PowderCell (version 2.3) [21].

Optical reflectance spectra were measured for $LiCu_2Al$ and $LiCu_2Ga$ from 200 nm (6.2 eV) to 1500 nm (0.83 eV) on an Agilent Cary 5000 UV–vis–NIR spectrophotometer equipped with a reflectance accessory. For comparison, spectra were also measured for elemental gold (99.999%, Materion) and various Au–Ag–Cu alloys that have been reported to be coloured and have been marketed commercially [1]. The alloys were prepared by reactions of the elemental components, which were arc-melted under an argon atmosphere in an Edmund Bühler MAM-1 arc melter. All samples were polished to obtain flat surfaces. The spectra were normalized, with a compacted pellet of $BaSO_4$ used as a 100% reflectance standard.

Magnetic measurements on ground, freshly synthesized samples were carried out on a Quantum Design 9T-PPMS magnetometer under an applied field of 3 T between 2 and 300 K. Magnetic susceptibility values were corrected for contributions from the sample holder.

Solid-state ^{7}Li nuclear magnetic resonance (NMR) spectra were acquired on a Bruker Avance 500 MHz (B_o = 11.75 T) NMR spectrometer equipped with a 4-mm magic angle spinning (MAS) probe operating in double resonance mode. Powdered samples were packed into 4-mm outside diameter ZrO_2 rotors with Kel-F caps; spectra were acquired on non-spinning samples. A Hahn echo pulse sequence with a 90° pulse width of 3.6 μs, an interpulse delay of 24.6 μs, and a recycle delay of 0.5 s were applied; 6400 to 13,100 transients were co-added. The spectra were referenced by setting the ^{7}Li peak of a 1.0-M LiCl(aq) solution to 0.0 ppm.

2.3. Electronic structure calculations

Pseudo-potential, first-principles electronic structure calculations were performed using the program Akai-KKR, with the Korringa-Kohn-Rostoker (KKR) Green function method combined with the local density approximation and the coherent potential approximation [22]. This method is suitable and convenient for structures exhibiting atomic disorder. To attain an accurate ground state, 400 *k*-points were used in the first Brillouin zone and the condition for convergence was set to 1×10^{-6} eV for the total energy.

3. Results and discussion

Initial investigations of the Li–Cu–*X* (*X* = group 13–15 metals or metalloids) system were carried out by high frequency induction melting of mixtures of the elements. They revealed that many samples with nominal composition $LiCu_2X$ exhibit colour. For example, $LiCu_2In$ and $LiCu_2Sb$ exhibit a golden yellow colour, but unfortunately the samples degrade rapidly in air. The most consistent results were obtained for $LiCu_2Al$ and $LiCu_2Ga$, which are reported here. Uniform, homogeneously melted, phase-pure samples with the most intense colours were obtained at optimized conditions of 157 kHz frequency, 138 A current, and 18 min heating time. $LiCu_2Al$ is red and $LiCu_2Ga$ is yellow. The colours remain intact for two to three days, gradually degrading so that the red colour of $LiCu_2Al$ turns to a darker shade and the yellow colour of $LiCu_2Ga$ fades. However, powder XRD patterns collected even after one year show virtually no change in the bulk samples (Figure S2 in Supplementary Data), implying that the colour degradation observed after a few days is probably a surface phenomenon.

The structures of these compounds were deduced from their powder XRD patterns, which are relatively simple (Fig. 1) and were indexed to cubic lattices (Table 1). $LiCu_2Al$ adopts a CsCl-type structure with a primitive cubic lattice (space group $Pm\bar{3}m$): Cu atoms occupy the 1*a* site at the corners of the unit cell, while Li and Al atoms are disordered over the 1*b* site at the centre of the unit cell (Fig. 2(a)). Following an alternative typical description of the CsCl-type structure, there are interpenetrating cubic arrays (not "lattices" or "sublattices," as sometimes described in the literature!) of Li/Al and Cu atoms. The XRD pattern of $LiCu_2Ga$ clearly shows additional peaks compared to that of $LiCu_2Al$ corresponding to a doubled unit cell length. $LiCu_2Ga$ adopts a Cu_2MnAl-type (full-Heusler) structure with a face-centred cubic lattice (space group $Fm\bar{3}m$): Cu atoms occupy the 8*c* site at ¼, ¼, ¼, while Li and Ga atoms are ordered over the 4*b* and 4*a* sites located at the edges, centre, and corners of the unit cell (Fig. 2(b)).

To complement the XRD results, and in particular, to confirm the occupation of Li atoms within one set of sites in the structures of $LiCu_2Al$ and $LiCu_2Ga$, solid state ^{7}Li NMR spectroscopy was also performed (Fig. 3). Magnetic measurements were first carried out to reveal that the samples are diamagnetic (Figure S1 in Supplementary Data) and thus contain no unpaired electrons, which would complicate the interpretation of the NMR spectra. The spectrum for $LiCu_2Al$ is dominated by a peak at 49 ppm, with a smaller peak (20% of the total intensity) at 0 ppm. The latter is typical of ionic Li, but the dominant peak is outside the typical Li chemical shift range, suggesting a Knight shift, a consequence of conduction electrons. Likewise, the ^{7}Li spectrum of $LiCu_2Ga$ is dominated by a peak at 48 ppm, with minor contributions totaling 5%, from peaks at 5 and 120 ppm. The occurrence of dominant peaks for both $LiCu_2Al$ and $LiCu_2Ga$ with the same chemical shift (within error) is consistent with the presence of similar chemical environments of eight nearest neighbour Cu atoms at 2.536–2.538 Å in a cubic geometry around the Li atoms in both structures. The ^{7}Li resonance for $LiCu_2Al$ (FWHM of 11 kHz) is significantly broader than that for $LiCu_2Ga$ (FWHM of 8 kHz), supporting the occurrence of Li/Al disorder in the former case, in which a random mixture of next-nearest neighbour Li and Al atoms in the second coordination sphere around each Li atom leads to a

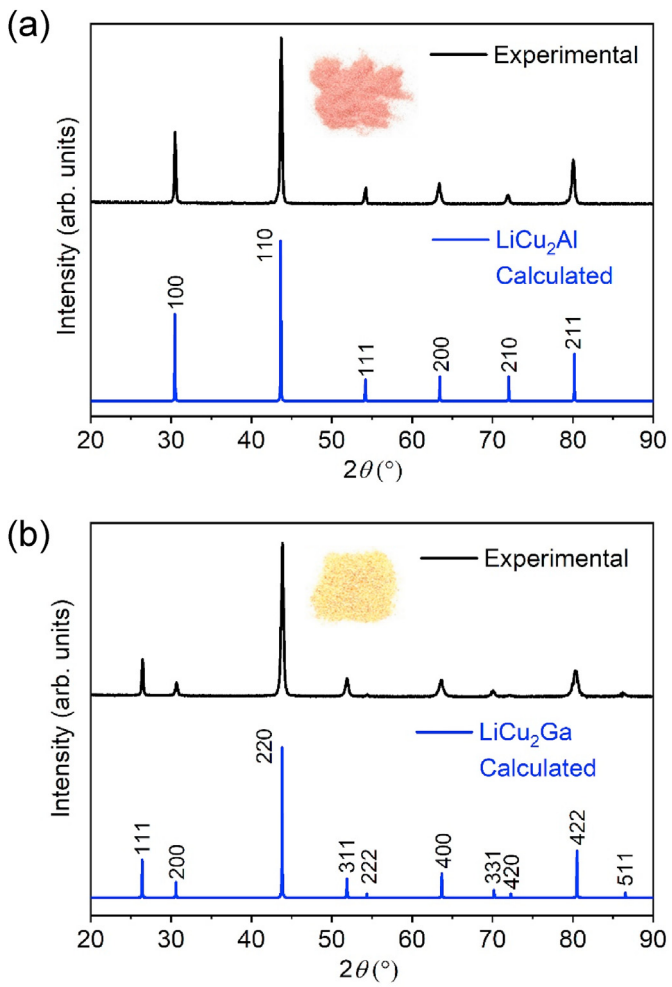

Fig. 1. Powder XRD patterns and images of powder samples for (a) $LiCu_2Al$ and (b) $LiCu_2Ga$.

Table 1
Crystallographic data for $LiCu_2Al$ and $LiCu_2Ga$.

Crystal data		
formula	$Li_{0.5}CuAl_{0.5}$	$LiCu_2Ga$
formula mass (amu)	80.51	203.76
space group	$Pm\bar{3}m$ (No. 221)	$Fm\bar{3}m$ (No. 225)
a (Å)	2.9283 (2)	5.8617 (4)
V (Å^3)	25.110 (5)	201.41 (4)
Z	1	4
ρ_{calcd} (g cm^{-3})	5.254	6.632
Atomic coordinates		
Li	Li at 1*b* (½, ½, ½), occ. 0.5	Li at 4*b* (½, ½, ½)
Cu	Cu at 1*a* (0, 0, 0)	Cu at 8*c* (¼, ¼, ¼)
X	Al at 1*b* (½, ½, ½), occ. 0.5	Ga at 4*a* (0, 0, 0)

broadening. The ^{7}Li resonances in $LiCu_2Al$ and $LiCu_2Ga$ are shifted to high frequency relative to those (−1.6 to 3.3 ppm) in the half-Heusler compounds Li*MPn* (*M* = Mg, Zn, Cd; *Pn* = P, As, Sb, Bi) [23]; as discussed above, the high frequency shifts for the compounds considered here are attributed to Knight shifts.

The optical reflectance spectra were measured on both ingot and powder samples. For $LiCu_2Al$, the spectra for the powder samples show somewhat different intensities; for $LiCu_2Ga$, the spectra are nearly the same for both types of samples (Figure S3 in Supplementary Data). The spectra of the powder samples tend to suffer from decreased reflectivity after a few days. If the analysis is restricted to ingot samples, these

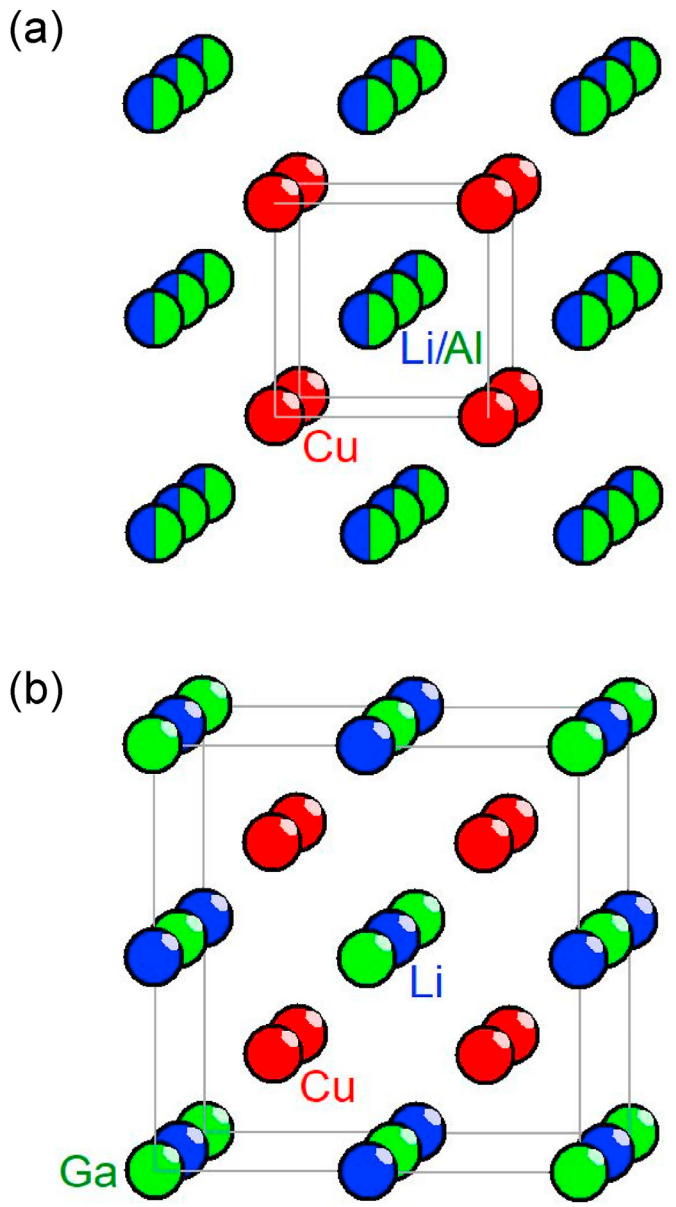

Fig. 2. Crystal structures of (a) $LiCu_2Al$ (CsCl-type) and (b) $LiCu_2Ga$ (Cu_2MnAl-type).

spectra are consistent with the colours observed for $LiCu_2Al$ and $LiCu_2Ga$, and can be compared with that for high purity (99.999%) Au (Fig. 4). In all cases, the reflectivity drops off abruptly at absorption edges of 2.4 eV for $LiCu_2Al$, 2.6 eV for Au, and 2.8 eV for $LiCu_2Ga$. The shift in absorption edge to higher energy agrees with the trend in colour, changing from red to yellow on progressing along this series. To assess the colours on more quantitative grounding, the optical reflectance was converted to coordinates in CIE 1931 colour space (with standard illuminant E) [24] and plotted on a chromaticity diagram (Fig. 5). The plot shows both ingot and powder samples of $LiCu_2Al$ and $LiCu_2Ga$, in comparison to pure gold as well as a variety of commercial coloured gold alloys that were synthesized in our laboratory according to their reported compositions (Table S2 in Supplementary Data). Despite the subjective terminology used to describe colours of gold alloys (e.g., green, yellow, rose, pink, red), their CIE *x* and *y* coordinates lie more or less within the same region of the diagram. An alternative interpretation is that human perception of colours is remarkably sensitive to small differences. $LiCu_2Al$ lies near the region of "pink" and $LiCu_2Ga$ near "orange" and "yellow" in this diagram. In particular, the colour coordinates for $LiCu_2Ga$ lie quite close to those

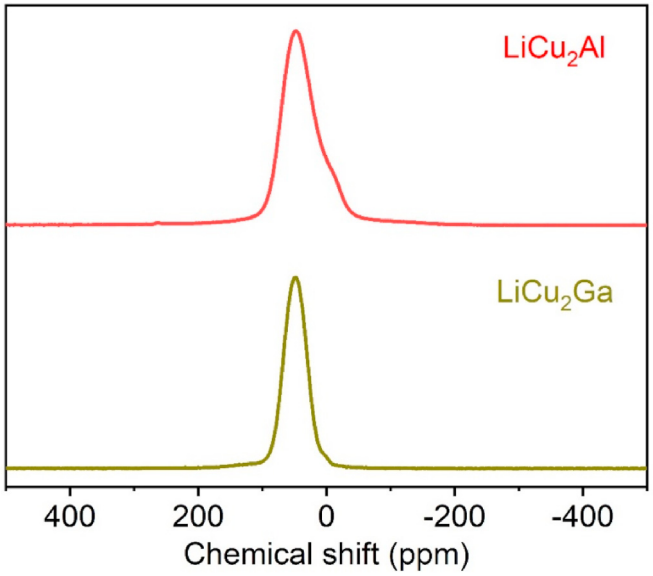

Fig. 3. ^{7}Li NMR spectra of $LiCu_2Al$ and $LiCu_2Ga$.

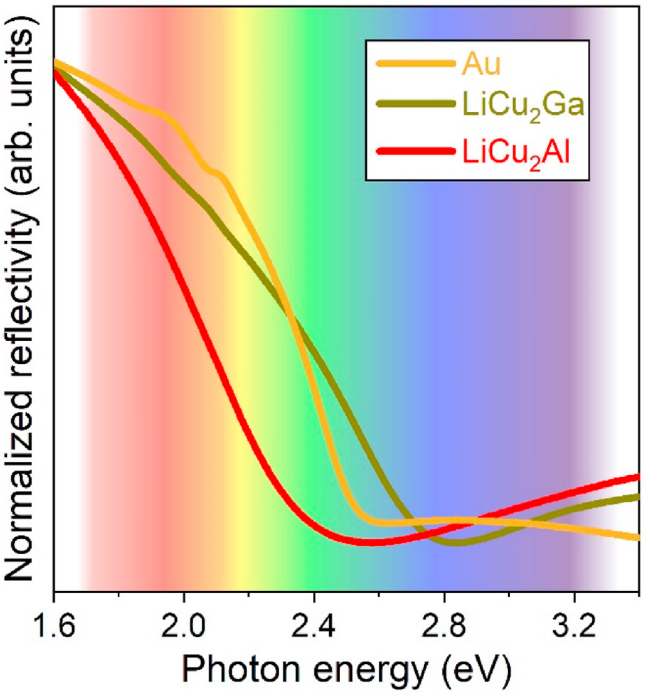

Fig. 4. Optical reflectivity spectra for ingots of $LiCu_2Al$, $LiCu_2Ga$, and high purity Au (99.999%).

for Au, consistent with their similar optical reflectivity profile. However, the average reflectance in the visible region is lower in $LiCu_2Ga$ (~22%) than Au (~50%).

The electronic structures of $LiCu_2Al$ and $LiCu_2Ga$ can be examined in more detail. Because $LiCu_2Al$ and $LiCu_2Ga$ are related to the family of Heusler and half-Heusler compounds, which have hybridization gaps resulting from a clear separation of bonding and antibonding states, it is tempting to propose charge-balanced formulations $(Li^{+})\ (Cu^{+})_2(Al^{3-})$ and $(Li^{+})\ (Cu^{+})_2(Ga^{3-})$ which would allow them to be classified as Zintl phases. However, this assumption would be problematic because the electronegativity of Cu is the greatest or similar to that of Ga (cf., Pauling, $\chi_{Cu} = 1.90$, $\chi_{Ga} = 1.81$; Allred-Rochow, $\chi_{Cu} = 1.75$, $\chi_{Ga} = 1.82$) among

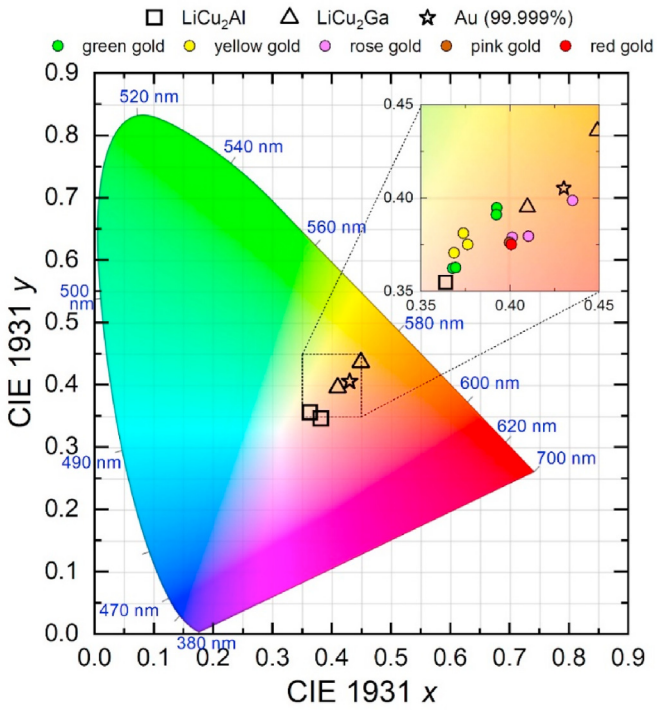

Fig. 5. CIE 1931 coordinates for $LiCu_2Al$, $LiCu_2Ga$, Au, and various commercially known coloured gold-containing alloys. (For interpretation of the references to colour in this figure legend, the reader is referred to the Web version of this article.)

the elemental components [25], so it is no longer clear if such valence rules apply in these compounds. Nevertheless, these compounds resemble the majority of other known coloured intermetallic compounds, generally ternary phases (Li or Mg)$-M-X$ (M = late transition metal; X = group [13–15] metal or metalloid) [16–19] for which an empirical rule has been proposed requiring a valence electron count of 7 or slightly less for colour to be exhibited [7,8]. For $LiCu_2Al$ and $LiCu_2Ga$, the electron count is 6 (per formula unit), which conforms to this electron counting rule.

From first-principles electronic structure calculations, the band dispersion diagrams for $LiCu_2Al$ and $LiCu_2Ga$ show a dense manifold of bands within a narrow energy range between −2.5 and −4.5 eV that originate from completely filled 3d states of the Cu atoms, overlaid on disperse bands resulting from mixing of Li 2s, Cu 4s/4p, and Al 3s/3p (or Ga 4s/4p) states (Fig. 6). The electronic structure lacks the feature of a pseudogap near the Fermi level characteristic of typical Zintl phases, and instead resembles that of elemental copper or gold [26,27]. The origin of colour in $LiCu_2Al$ and $LiCu_2Ga$ is thus similar to that of copper or gold [28], namely interband transitions from the filled Cu 3d states to the continuum of empty states above the Fermi level. The top of the Cu 3d band lies at about 2.5 eV below the Fermi level, in reasonably good agreement with the absorption edges of 2.4 eV for $LiCu_2Al$ and 2.8 eV for $LiCu_2Ga$ observed in the optical reflectance spectra.

4. Conclusions

$LiCu_2Al$ and $LiCu_2Ga$ were identified as unusual examples, still few, of intermetallic compounds that exhibit colour. Of these two compounds, $LiCu_2Ga$ is perhaps most interesting because its yellow colour resembles that of elemental gold, as confirmed by their optical reflectance spectra and quantification of CIE colour coordinates. The origin of the colour can be traced to electronic transitions from narrow, completely filled bands based on Cu 3d states to empty states above the Fermi level.

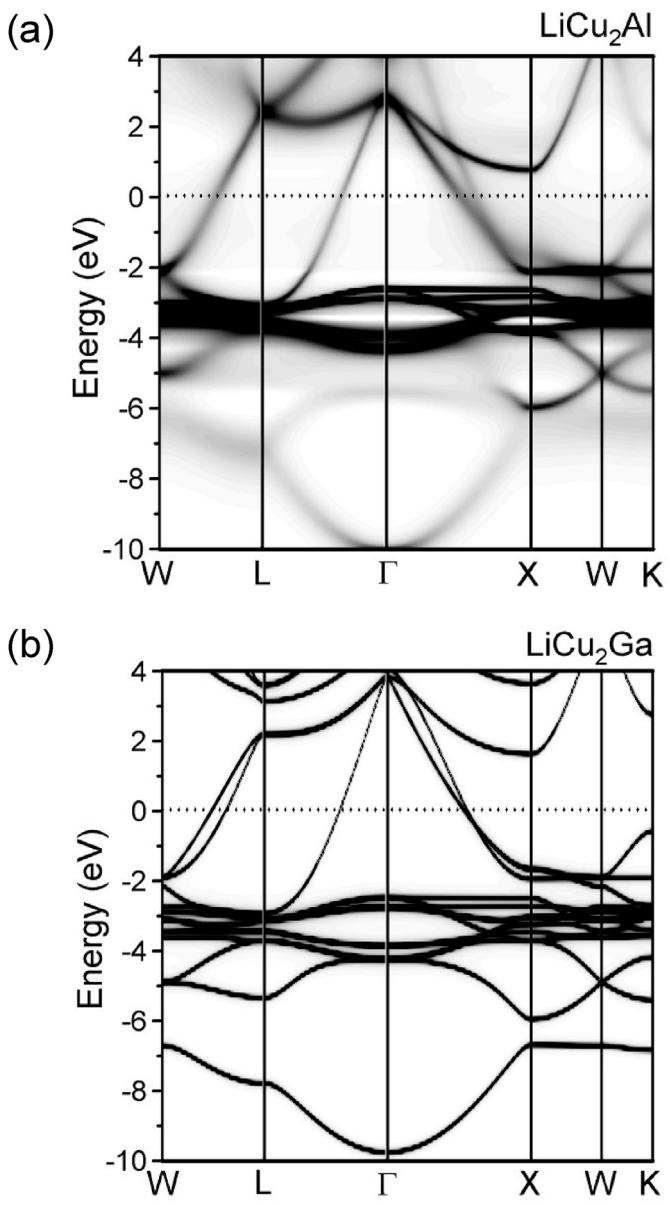

Fig. 6. Band dispersion for (a) $LiCu_2Al$ and (b) $LiCu_2Ga$. In (a), the degree of blurring indicates states that are most strongly affected by disorder of Li and Al atoms in the crystal structure.

CRediT authorship contribution statement

Vidyanshu Mishra: Formal analysis, Investigation, Writing - original draft. **Abishek K. Iyer:** Conceptualization, Methodology, Formal analysis, Investigation, Writing - review & editing. **Dundappa Mumbaraddi:** Formal analysis, Investigation. **Anton O. Oliynyk:** Formal analysis. **Guillaume Zuber:** Investigation. **Aurélien Boucheron:** Investigation. **Grygoriy Dmytriv:** Investigation. **Guy M. Bernard:** Investigation. **Vladimir K. Michaelis:** Formal analysis. **Arthur Mar:** Conceptualization, Formal analysis, Writing - original draft.

Declaration of competing interest

The authors declare that they have no known competing financial interests or personal relationships that could have appeared to influence the work reported in this paper.

Acknowledgments

This work was supported by the Natural Sciences and Engineering Research Council of Canada (NSERC, through Discovery Grant RGPIN-2018-04294) and the NSERC Collaborative Research and Training Experience Program (CREATE, through the Alberta/Technical University of Munich International Graduate School (ATUMS)).

Appendix A. Supplementary data

Supplementary data to this article can be found online at https://doi.org/10.1016/j.jssc.2020.121703.

References

[1] C. Cretu, E. van der Lingen, Coloured gold alloys, Gold Bull. 32 (1999) 115–126.
[2] I.M. Wolff, Spangold: a new aura for intermetallics, Endeavour 19 (1995) 16–19.
[3] C.W. Corti, Black, blue and purple! the special colours of gold, , in: E. Bell (Ed.), The Santa Fe Symposium on Jewelry Manufacturing Technology, , Met-Chem Research, Albuquerque, 2004, pp. 121–134.
[4] U.E. Klotz, Metallurgy and processing of coloured gold intermetallics – Part I: properties and surface processing, Gold Bull. 43 (2010) 4–10.
[5] J. Fischer-Bühner, A. Basso, M. Poliero, Metallurgy and processing of coloured gold intermetallics – Part II: investment casting and related alloy design, Gold Bull. 43 (2010) 11–20.
[6] J. Liu, Y. Liu, P. Gong, Y. Li, K.M. Moore, E. Scanley, F. Walker, C.C. Broadbridge, J. Schroers, Combinatorial exploration of color in gold-based alloys, Gold Bull. 48 (2015) 111–118.
[7] S.G. Steinemann, W. Wolf, R. Podloucky, Color and optical properties, Principles and Practice, in: J.H. Westbrook, R.L. Fleischer (Eds.), Intermetallic Compounds, vol. 3 Wiley, New York, 2002, pp. 231–244.
[8] E. van der Lingen, Aspects of coloured precious metal intermetallic compounds, J. S. Afr. Inst. Min. Metall. 114 (2014) 137–144.
[9] S.G. Steinemann, P.N.B. Anongba, R. Podloucky, Color in Pettifor's structure maps: intermetallic compounds for a new use, J. Phase Equil. 18 (1997) 655–662.
[10] R.W. Cahn, A precious stone that isn't, Nature 396 (1998) 523–524.
[11] V.J. Keast, K. Birt, C.T. Koch, S. Supansomboon, M.B. Cortie, The role of plasmons and interband transitions in the colour of $AuAl_2$, $AuIn_2$, and $AuGa_2$, Appl. Phys. Lett. 99 (2011) 111908-1–111908-3.
[12] A. Furrer, M. Seita, R. Spolenak, The effects of defects in purple $AuAl_2$ thin films, Acta Mater. 61 (2013) 2874–2883.
[13] J. Hurly, P.T. Wedepohl, Optical properties of coloured platinum intermetallic compounds, J. Mater. Sci. 28 (1993) 5648–5653.
[14] L.V. Nomerovannaya, M.M. Kirillova, A.B. Shaikin, Interband absorption in the coloured intermetallic compounds PdIn, Phys. Status Solidi B 102 (1980) 715–720.
[15] Y.B. Jeong, J.T. Kim, S.H. Hong, H.D. Lee, S.Y. Choi, K.B. Kim, Compositional tuning-induced permanent color adjustment and mechanical properties: binary Cu–Mg colored metallic system, Mater. Des. 175 (2019) 107814-1–107814-11.
[16] U. Eberz, W. Seelentag, H.-U. Schuster, Zur Kenntnis farbiger ternärer und quaternärer Zintl-Phasen, Z. Naturforsch. B Chem. Sci. 35 (1990) 1341–1343.
[17] J. Drews, U. Eberz, H.-U. Schuster, Optische Untersuchungen an farbigen intermetallischen Phasen, J. Less Common. Met. 116 (1986) 271–278.
[18] A. Czybulka, A. Petersen, H.-U. Schuster, Lithium–Platinmetall–Al(Ga,In)-Legierungen: neue farbige ternäre intermetallische Phasen, J. Less Common. Met. 161 (1990) 303–312.
[19] G. Dymtriv, H. Pauly, H. Ehrenberg, V. Pavlyuk, E. Vollmar, Homogeneity range of the NaTl-type Zintl phase in the ternary system Li–In–Ag, J. Solid State Chem. 178 (2005) 2825–2831.
[20] P. Villars, K. Cenzual, Pearson's Crystal Data – Crystal Structure Database for Inorganic Compounds (On DVD), Release, ASM International, Materials Park, OH, USA, 2019.
[21] W. Kraus, G. Nolze, Powder cell - a program for the representation and manipulation of crystal structures and calculation of the resulting X-ray powder patterns, J. Appl. Crystallogr. 29 (1996) 301–303.
[22] N.H. Long, H. Akai, First-principles KKR-CPA calculation of interactions between concentration fluctuations, J. Phys. Condens. Matter 19 (2007) 365232-1–365232-8.
[23] S. Dupke, H. Eckert, F. Winter, R. Pöttgen, A systematic solid state NMR spectroscopic study of the equiatomic lithium half-Heusler phases Li*TX* (*T* = Mg, Zn, Cd; *X* = P, As, Sb, Bi), Prog. Solid State Chem. 42 (2014) 57–64.
[24] R.W.G. Hunt, M.R. Pointer, Measuring Colour, fourth ed., Wiley, Chichester, 2011.
[25] J.E. Huheey, E.A. Keiter, R.L. Keiter, Inorganic Chemistry: Principles of Structure and Reactivity, fourth ed., Harper Collins, New York, 1993.
[26] G.A. Burdick, Energy band structure of copper, Phys. Rev. 129 (1963) 138–150.
[27] T. Rangel, D. Kecik, P.E. Trevisanutto, G.-M. Rignanese, H. Van Swygenhoven, V. Olevano, The bandstructure of gold from many-body perturbation theory, Phys. Rev. B 86 (2012) 125125-1–125125-10.
[28] K.E. Saeger, J. Rodies, The colour of gold and its alloys, Gold Bull. 10 (1977) 10–14.